Scientific Research Publishing

Open Journal of Composite Materials, 2025, 15(1), 44-57
https://www.scirp.org/journal/ojcm
ISSN Online: 2164-5655
ISSN Print: 2164-5612

Fully Recycled Syntheses Using Recycled Concrete Powder, Oyster Shell and Wood Powder: Effect of Combined Ground Treatment on Mechanical Strength and FTIR, XRD, and SEM Characterization

Ejazulhaq Rahimi*, Yuma Kawasaki, Ayane Yui, Yuta Yamachi

Department of Civil and Environmental Engineering, Ritsumeikan University, Kusatsu, Japan
Email: *gr0448vi@ed.ritsumei.ac.jp

How to cite this paper: Rahimi, E., Kawasaki, Y., Yui, A. and Yamachi, Y. (2025) Fully Recycled Syntheses Using Recycled Concrete Powder, Oyster Shell and Wood Powder: Effect of Combined Ground Treatment on Mechanical Strength and FTIR, XRD, and SEM Characterization. *Open Journal of Composite Materials*, **15**, 44-57.
https://doi.org/10.4236/ojcm.2025.151003

Received: November 11, 2024
Accepted: January 4, 2025
Published: January 7, 2025

Abstract

The use of recycled concrete and oyster shells as partial cement and aggregate replacements is ongoing research to solve this multifaceted problem of concrete waste in the construction industry as well as waste from oyster shell farming. However, there is a lack of evidence on the possibility of producing a fully recycled composite consisting of recycled concrete and oyster shell without the need for new cement and natural aggregates. In this study, recycled concrete powder (RCP) and oyster shell were used to produce a green composite. Separate ground and combined ground (separate ground and co-ground) RCP and oyster shells are used to determine the effects of grinding approaches on the mechanical and chemical properties of the composite. The composite samples were molded via press molding by applying 30 MPa of pressure for 10 minutes. The results revealed that the composite prepared via the combined ground approach presented the highest flexural strength compared to the separate ground and unground samples. The FTIR and XRD characterization results revealed no chemical or phase alterations in the raw materials or the resulting composites before and after grinding. SEM analysis revealed that combined grinding reduced the particles' size and improved the dispersion of the mixture, thereby increasing the strength.

Keywords

Oyster Shells, Grinding, Recycled Concrete Powder, Waste Wood, Composite

1. Introduction

The generation of large amounts of construction and demolition waste poses great environmental challenges, as only in 40 countries did the annual generation of waste reach 3 billion tons until 2012 [1]. This highlights the importance of recycling waste, which is generated at the expense of $CaCO_3$ and natural aggregate exploitation, to produce cement and concrete. The present evidence shows that recycled concrete is mainly used for preparing recycled coarse aggregate for use in concrete [2]-[4] and roadway construction [5]-[7]. Additionally, the RCP generated during concrete recycling is mainly used for partial cement replacement [8]-[10] and fine aggregate replacement [11]-[13] in conventional and geopolymer concretes. The utilization of RCP with the current approaches does not fully replace cement and still requires additional cement to new concrete production. In addition, according to the literature, since the strength of recycled aggregates decreases during subsequent recycling, concrete can be recycled and reused only a finite number of times [14]. Therefore, the complete circle of recycling in concrete in a sustainable way is still elusive, which encourages investigations to determine other possible ways to recycle and reuse concrete.

Furthermore, as another waste, oyster shells are a byproduct of shelled oysters, which their production is increasing worldwide. In 2020, 6.06 million tons of live oysters were produced worldwide [15]. Oyster shells account for approximately 90% of the total oyster mass, contributing to the generation of a large amount of waste [16], which needs to be handled sustainably. A number of studies have shown promising evidence for recycling oyster shells for new concrete production. In particular, they have shown that seashells, including oysters, can be used as either aggregates [17]-[19] or partial cement replacements [20]-[22]. In the former, the oyster shell is calcined or ground and added to the cement, resulting in increased concrete strength as it replaces a certain amount of cement. Since oyster shells contain approximately 90% $CaCO_3$, their incorporation into concrete contributes to $CaCO_3$ resource conservation. The latter approach contributes to sand resource conservation by replacing the sand used for concrete production [23]. However, both waste recycling and reusing do not fully replace either cement or aggregates. Additionally, no studies in literature have investigated the possibility of preparing a composite using only RCP and oyster shell combinations and revealed their synergistic effects on the properties of a non-cement composite.

The present research aims to develop a composite using RCP and oyster shells via ball milling and press molding approaches. To unveil the different effects of griding approaches, separate grinding and combined grinding is compared. To highlight the effectiveness and consistency of the method, oyster shells are replaced with waste wood, and the strength of the wood-based composite is compared with that of the oyster shell-based samples. The results of the study introduce an approach that could contribute to making high value and efficient use of waste and have positive ecological and economic benefits.

2. Materials and Methods

2.1. Raw Materials

The raw materials used in this experiment are shown in Figure 1. To prepare the non-cement composite, the experiments used RCP, wood sawdust, and oyster shell, which were procured from local sources and oven dried for 24 hours at 120˚C. The dried RCP was sieved through a 0.3 mm sieve, but the wood powder and oyster shell powder were sieved through a 0.6 mm sieve and stored in sealed bags before the experiment.

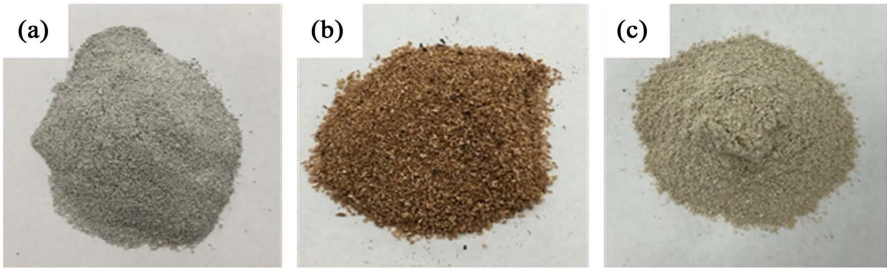

Figure 1. Materials: (a) RCP; (b) Wood powder; (c) Oyster shells.

2.2. Experimental Procedure

The experimental plan is shown in Table 1. It consists of three cases. In case 1, in a plastic container, unground RCP and oyster shell were mixed for 1 minute under dry conditions, and then, the water was added to the mixture and mixed for one more minute manually. The mixture was subjected to pressure at 30 MPa for 10 minutes using an AS ONE H400-15 hot-pressing machine and subsequently demolded, which yielded a hardened body, which was labeled the RCP-OS-UG sample. The molding procedure and apparatus are shown in Figure 2. It is mentioned that this experiment used a cold press, and no heat was applied.

Table 1. Materials and conditions.

Case	Materials (gr)				Treatment		Molding condition	
	RCP	W	OS	Water	Separate ground (min)	Co-ground (min)	Pressure (MPa)	Pressing time (min)
1	12	6	-	3	-	-	30	10
	12	-	6	3				
2	12	6	-	3	5	-		
	12	-	6	3				
3	12	6	-	3	5	2		
	12	-	6	3				

W: wood powder; OS: osyter shells.

For cases 2 and 3, a mixer mill (MM400, Retsch) was used to grind the raw materials using 50 ml jar and 25 mm ball diameter with a 25 Hz horizontal

oscillation frequency.

In case 2, the RCP and oyster shell samples were separately ground for five minutes. The ground materials were poured into a plastic container and mixed for one minute. Then, water was added to the mixture, which was mixed for one more minute. Finally, the mixture was molded under the same conditions as those in case 1, and the obtained sample was marked as RCP-OS-SG.

In case 3, first, RCP and oyster shells were ground separately for five minutes, resulting in fine powders. The powders were subsequently mixed and ground for 2 minutes via the same ball mill machine. This is called combined ground. Next, water was added to the mixture, which was mixed for one minute in a plastic container. Finally, the molding activity was performed under the same conditions as mentioned above.

Similarly, the above procedures were applied to RCP and wood for the three cases, in which only cases 2 and 3 produced hardened bodies. However, in case 1, the mixture could not harden, and thus, no sample was obtained.

Notably, the unground, separate ground and combined ground average particle sizes were measured via SYNC and a NANOTRAC WAVE II Microtrac particle size analyzer. For the particle size measurement of case 3, individual raw materials were ground in two steps, first for five minutes and then for two minutes without mixing, to measure the individual material particle size instead of the mixture size.

All the samples were cured at room temperature for 72 hours before conducting a flexural test.

2.3. Experimental Investigations

After obtaining the samples and conducting the flexural strength test the samples were characterized using the following analytical methods to illustrate the microstructure and the possible chemical alteration during grinding.

2.3.1. X-Ray Diffraction Analysis

Mineral composition analysis was conducted via an XRD diffractometer (D8 DISCOVER, Bruker) operating at 40 kV and 40 mA with Cu-Kα radiation. The scanning step size was set to 0.02˚ in the 2θ range of 10˚ to 70˚. The XRD was employed to examine the mineral composition of the samples prepared from unground, separate ground and combined ground samples.

2.3.2. FTIR Spectral Analysis

FTIR spectra were acquired using a PerkinElmer Spectrum 3 instrument. The spectra were recorded over a range of 4000 - 400 cm^{-1} with a resolution of 4 cm^{-1}. The data of the samples containing RCP were normalized to the peak at 874 out-of-plane vibrations of C-O in the pure RCP spectra.

2.3.3. Microstructural Analysis

The microstructures of the composite samples were analyzed by SEM–EDS via a FlexSEM1000II microscope to 1) Characterize the structural features of the

composite; 2) Determine the elemental composition and distribution of the samples through elemental mapping; 3) Assess the morphological characteristics of the samples.

3. Results and Discussions

3.1. Influence of Grinding on Particle Size and Strength Development

The particle size of the particulates is shown in Figure 2. The unground average particle sizes of RCP, oyster shell, and wood are 215, 340, and 368 μm, respectively. After separate grinding, the size decreased to 92, 54, and 117 μm, and after combined grinding, the size further decreased to 52, 39, and 72 μm. The effects of particle size and grinding method on the flexural strength of oyster shell-based samples and wood-based samples are shown in Figure 3. As shown in Figure 3, the composite made of unground RCP and wood powder did not harden, but the composite made of unground RCP and oyster shell powder hardened and had a 0.9 MPa flexural strength. In case 2, when the materials were separately ground for five minutes and their particle sizes decreased, both the oyster-based and the wood-based composites hardened and demonstrated flexural strengths of 1.2 MPa and 0.8 MPa, respectively, confirming the findings of previous studies that indicate an inverse relationship between the size of oyster shell particles and concrete strength [24] [25]. In case 3, when combined ground was applied, the composite flexural strength increased to 4.3 MPa and 1.6 MPa in both oyster shell and wood-based composites, showing 258% and 100% enhancement, respectively. According to Erdugdo *et al.* [26], co-gripping leads to strength improvement, which is associated with a reduction in the particle size and homogeneity of the mixture. This result is also consistent with the findings of Onaizi *et al.* [27] and Dvořák *et al.* [28], who reported that co-ground samples presented a greater increase in strength at an early age than did those containing the equivalent ratios of mixtures ground separately.

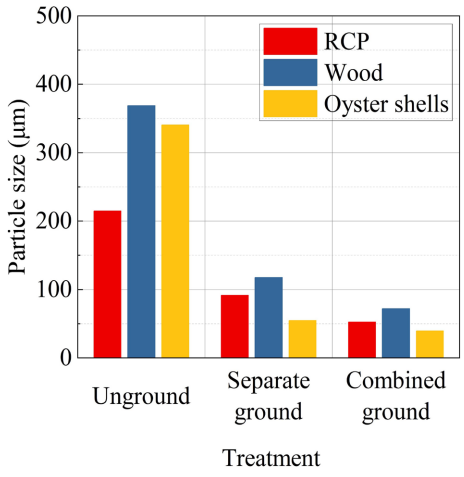

Figure 2. Particle size of RCP, wood, and oyster shell.

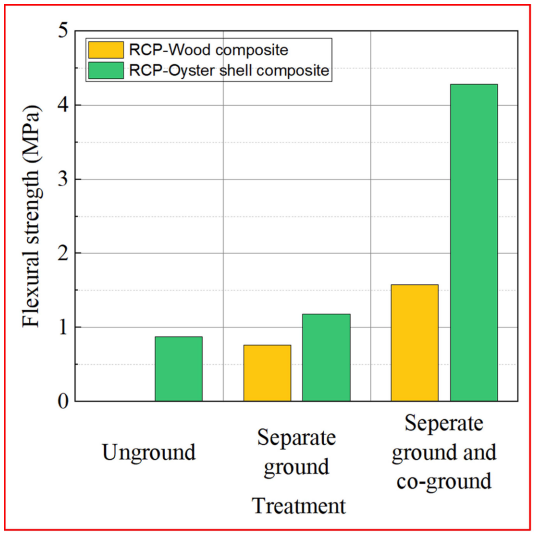

Figure 3. Flexural strength of the RCP-oyster shell and RCP-wood samples.

3.2. Influence Grinding on Chemical and Structural Phases

The X-ray diffraction (XRD) patterns of the unground, separately ground, combined ground samples, and RCP, oyster shell, and wood are shown in **Figure 4** and **Figure 5**. In RCP, the XRD peaks mostly indicate the presence of $CaCO_3$ and SiO_2. This also indicates the availability of $Ca(OH)_2$. In oyster shells, since oysters abundantly contain $CaCO_3$, the peaks are solely indicative of the existence of $CaCO_3$. The XRD patterns of the unground, separately ground, and combined ground samples display overlapping features, with no significant deviations between the individual patterns. This finding indicates that the grinding process does not substantially alter the material phases, which aligns with the findings of Onaizi *et al.* [27], who reported that co-grinding does not lead to structural transformations in the powder or induce the formation of new phases.

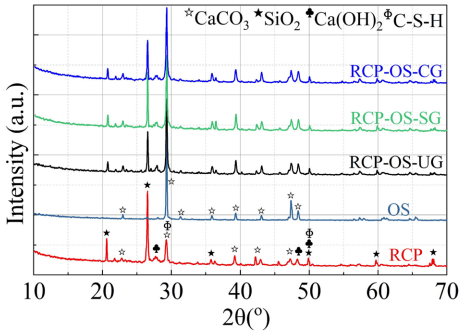

Figure 4. XRD pattern of RCP-oyster shells samples.

The FTIR spectra in the frequency range of 4000 - 400 cm^{-1} for the materials and the composite samples from the unground, separate ground, and combined ground samples, and RCP, oyster shell, and wood are shown in **Figure 6** and **Figure 7**. For both the RCP-oyster shells and RCP-wood samples, the figures indicate

that the major peaks for all the samples (unground, separate ground and co-ground) appear at approximately 3438, 2514, 1798, 1420, 1011, 874, and 713 cm^{-1}.

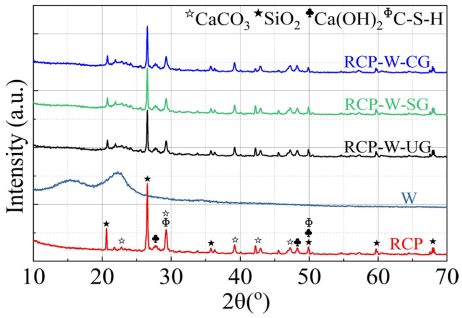

Figure 5. XRD pattern of RCP-wood samples.

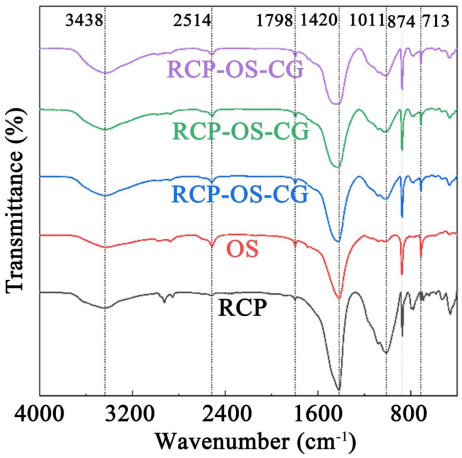

Figure 6. FTIR spectra of RCP-oyster shells samples.

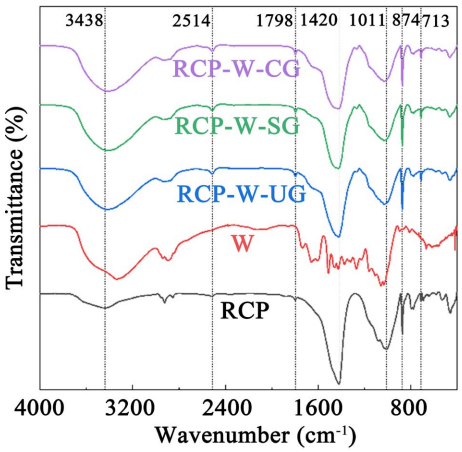

Figure 7. FTIR spectra of RCP-wood samples.

As shown in Table 2, the peak at 3438 cm^{-1}, which is related to O-H bending and vibrations, arises from water adsorbed on the surface of the samples and the hydration products of C_3S and C_2S [29] [30]. The peaks at 2514 and 1798 cm^{-1} correspond to $CaCO_3$ [31] [32]. The peak at 1420 cm^{-1} indicates the asymmetric

C-O stretching of carbonate molecules, which results from calcium hydroxide carbonation [30] [33]. The peak at 1011 cm^{-1} corresponds to Si-O asymmetric stretching and is due to the formation of hydraulic compounds such as C-S-H [30] [33]. The peak at 874 cm^{-1} shows the out-of-plane vibration of C-O in $CaCO_3$ [33] [34]. The peak at 713 cm^{-1} indicates the in-plane vibration of the C-O of $CaCO_3$ [33].

No new peak appeared or disappeared or shifted in any of the three cases, which is consistent with the XRD results and showed that there is no chemical alteration or new phase formation when the raw materials are ground separately or in combination.

Table 2. Summarized data of **Figure 6** and **Figure 7**.

Wavenumber [cm^{-1}]	Functional bond	Assigned to	Reference
3438	Stretching vibration of O-H	H_2O, $Ca(OH)_2$	[29]
2514		$CaCO_3$	[31] [32]
1798		$CaCO_3$	[31]
1420	Asymmetric C-O stretching	$CaCO_3$	[33] [35]
1011	Si-O asymmetric stretching	C-S-H	[31] [33]
874	Out of plane vibration of C-O	$CaCO_3$	[33]
713	In-plane vibration of C-O	$CaCO_3$	[33]

3.3. Influence of Grinding on Microstructures

Figure 8 and **Figure 9** show SEM images of RCP-oyster shells and RCP-wood samples made of the unground, separate ground and combined ground raw materials. As shown in the figures, the size of the particles and voids decreased from the unground samples to the combined ground samples. RCP-OS-CG shows significantly denser microstructures. In contrast, the samples in RCP-OS-SG, which were prepared with separately ground RCP and oyster shell mixtures, were less homogeneous and had more porous microstructures. Compared with the RCP-OS-SG samples, the homogeneous and compacted microstructure of the RCP-OS-CG case considerably contributed to its better flexural strength. Similarly, unlike the RCP-OS-SG sample, the RCP-OS-CG samples exhibited a more uniform dispersion of particles. This may be due to the synergistic effect and fineness achieved by the combined grinding of the RCP and oyster shell or wood combination. The same characterization can be seen in the cases of RCP-W-UG, RCP-W-SG, and RCP-W-CG. The results are in accordance with the results of Onaizi *et al.* [27], who reported that the co-ground effectively fills voids and transition zones between particles.

Table 3 shows the EDS data of the RCP-OS-UG, RCP-OS-SG, and RCP-OS-CG samples. The elemental compositions were obtained via SEM–EDS by mapping analysis of the surface of the samples. The major elements in the samples were O, C, and Ca, which indicate the abundance of $CaCO_3$ in the samples. The O and Ca contents decreased from the unground samples to the combined ground one. However, the C, Si, Al, and Na contents increased from the unground

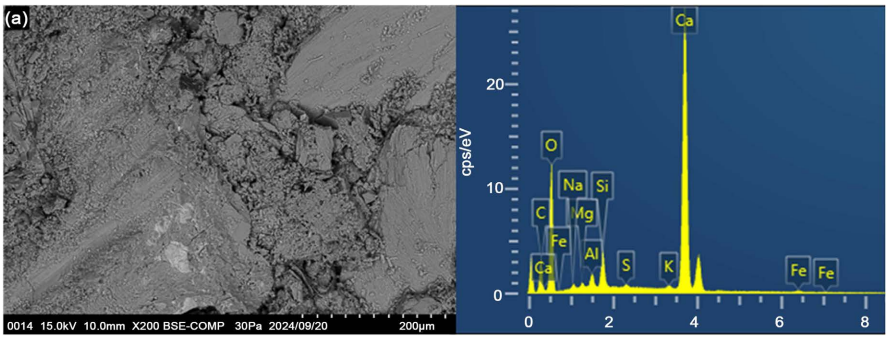

(a)

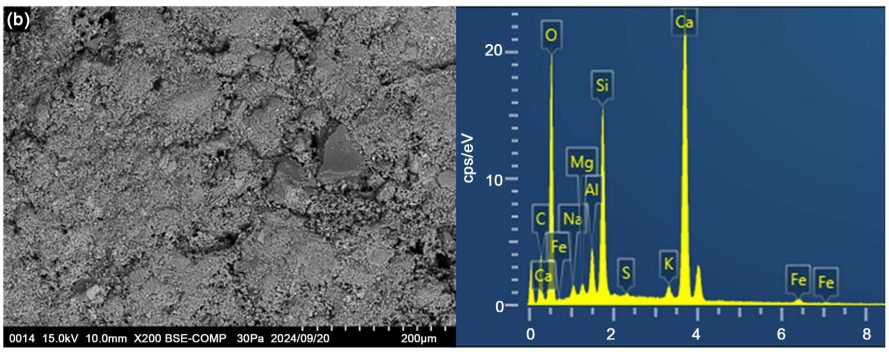

(b)

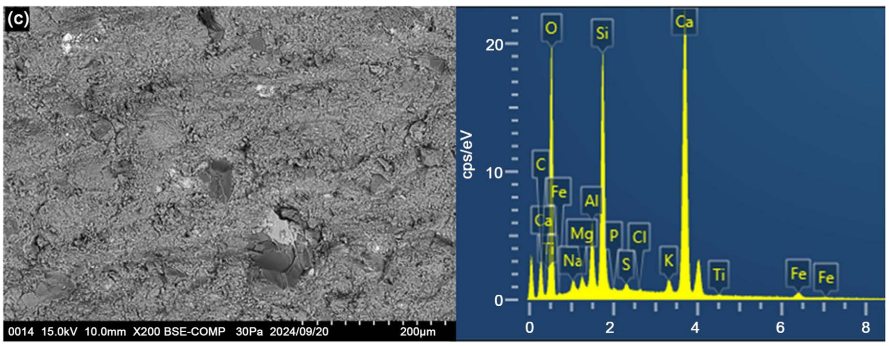

(c)

Figure 8. SEM micrographs of RCP-oyster shells samples: (a) RCP-OS-UG; (b) RCP-OS-SG; (c) RCP-OS-CG.

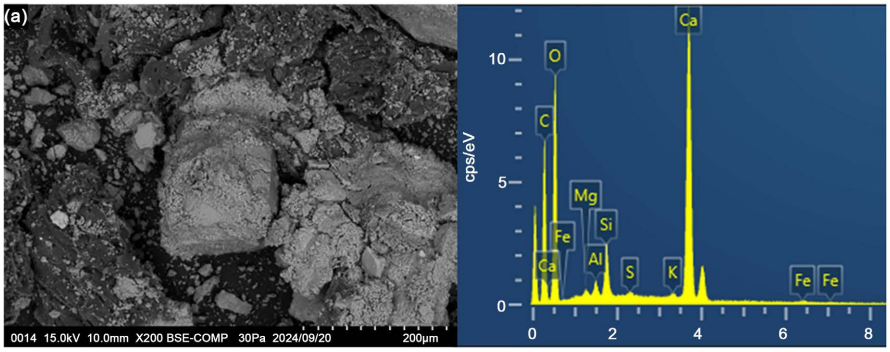

(a)

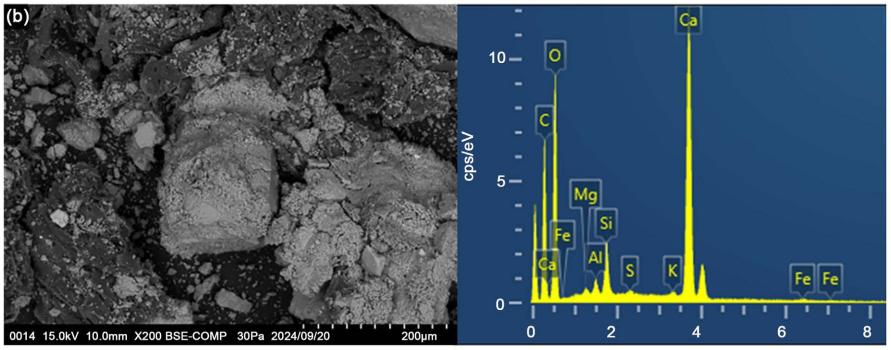

(b)

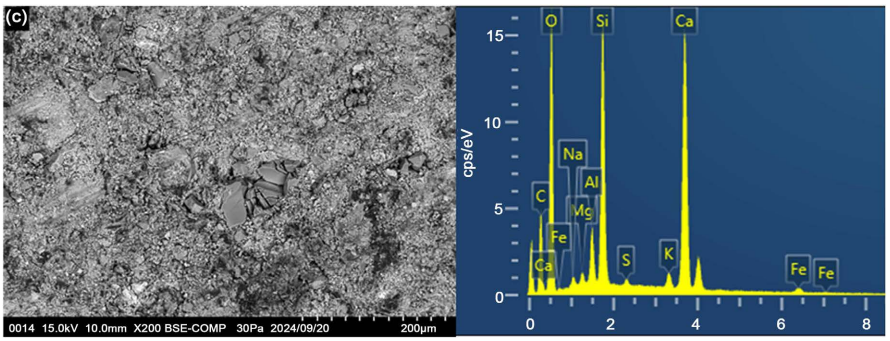

(c)

Figure 9. SEM micrographs of RCP-wood samples: (a) RCP-W-UG; (b) RCP-W-SG; (c) RCP-W-CG.

samples towards the combined ground samples. The difference in percentage increase was significant between the unground and separate ground samples but was not significant between the separate ground and combined ground samples. Considering the element ratios, the Ca/Si and Ca/Na ratios decreased after grinding. However, the Si/Al ratio increased. Nukah *et al.* studied the reduction in calcium in ground granular blast furnace slag (GGBS), and increasing the amount of silica improved the mechanical strength [36].

Table 3. Atomic percentages and ratios of hardened oyster shell and RCP based on EDS analyses.

Atom percentage and ratios	RCP-OS-UG (Figure 8(a))	RCP-OS-SG (Figure 8(b))	RCP-OS-CG (Figure 8(c))
O%	57.59	56.25	55.42
C%	20.67	23.7	22.66
Ca%	18.27	11.7	11.31
Si%	1.6	5.13	6.45
Al%	0.65	1.36	1.86
Na%	0.39	0.58	0.56
Ca/Si	11.42	2.28	1.75
Ca/Na	46.85	20.17	20.20
Si/Al	2.46	3.77	3.47

These results are in accordance with those of previous studies. A reduction in the Ca/Si ratio increased the compressive strength of the cementitious calcium-silicate-hydrate mixture [37]. Co-grinding decreased the Ca/Si ratio and increased the strength of the concrete [27]. Dinh *et al.* studied fly ash-based geopolymer concrete and reported that a Si/Al ratio in the range of 1.5 - 5 increased the compressive strength [38]. Kunther *et al.* reported that in calcium silicate hydrate binder (C-S-H), the higher the Ca/Si ratio is, the lower the strength, and the lower the Ca/Si ratio is, the higher the strength [37].

4. Conclusion

In this research, the influences of separate grinding and combined grinding (separate ground and co-ground) of RCP and oyster shells and RCP and wood powder on the flexural strength of samples of different combinations were investigated. The possibility of chemical reactions occurring by grinding was investigated via FTIR and XRD analyses, and the morphological structures of the samples were studied via SEM. The current study highlights several points, which can be summarized as follows:

- The synthesis used the combined ground RCP and oyster shell powder, which showed greater flexural strength than the use of only separate ground.
- The XRD patterns and FTIR spectra of the unground, separate ground and combined ground RCP and oyster shell or wood combinations display merged characteristics from the individual patterns of both RCP and oyster shell or wood, without any notable deviations, and indicate that no chemical alterations or phase changes occurred during grinding.
- Microstructural analyses revealed denser and more compact microstructures in the samples from the combined ground RCP and oyster shell or wood combinations, along with lower Ca/Si and Si/Al ratios, indicating the positive influence of these factors on the composite mechanical strength.

Acknowledgements

The authors acknowledge the financial support of the Heisie Kogyo and Amano Institute of Technology.

Conflicts of Interest

The authors declare no conflicts of interest regarding the publication of this paper.

References

[1] Akhtar, A. and Sarmah, A.K. (2018) Construction and Demolition Waste Generation and Properties of Recycled Aggregate Concrete: A Global Perspective. *Journal of Cleaner Production*, **186**, 262-281. https://doi.org/10.1016/j.jclepro.2018.03.085

[2] Wang, B., Yan, L., Fu, Q. and Kasal, B. (2021) A Comprehensive Review on Recycled Aggregate and Recycled Aggregate Concrete. *Resources, Conservation and Recycling*, **171**, Article ID: 105565. https://doi.org/10.1016/j.resconrec.2021.105565

[3] Guo, H., Shi, C., Guan, X., Zhu, J., Ding, Y., Ling, T., *et al.* (2018) Durability of

Recycled Aggregate Concrete—A Review. *Cement and Concrete Composites*, **89**, 251-259. https://doi.org/10.1016/j.cemconcomp.2018.03.008

[4] Verian, K.P., Ashraf, W. and Cao, Y. (2018) Properties of Recycled Concrete Aggregate and Their Influence in New Concrete Production. *Resources, Conservation and Recycling*, **133**, 30-49. https://doi.org/10.1016/j.resconrec.2018.02.005

[5] Xu, X., Luo, Y., Sreeram, A., Wu, Q., Chen, G., Cheng, S., *et al.* (2022) Potential Use of Recycled Concrete Aggregate (RCA) for Sustainable Asphalt Pavements of the Future: A State-Of-The-Art Review. *Journal of Cleaner Production*, **344**, Article ID: 130893. https://doi.org/10.1016/j.jclepro.2022.130893

[6] Loureiro, C.D.A., Moura, C.F.N., Rodrigues, M., Martinho, F.C.G., Silva, H.M.R.D. and Oliveira, J.R.M. (2022) Steel Slag and Recycled Concrete Aggregates: Replacing Quarries to Supply Sustainable Materials for the Asphalt Paving Industry. *Sustainability*, **14**, Article 5022. https://doi.org/10.3390/su14095022

[7] Jaawani, S., Franco, A., De Luca, G., Coppola, O. and Bonati, A. (2021) Limitations on the Use of Recycled Asphalt Pavement in Structural Concrete. *Applied Sciences*, **11**, Article 10901. https://doi.org/10.3390/app112210901

[8] Wu, H., Liu, C., Zhao, Y., Chen, G. and Gao, J. (2024) Elucidating the Role of Recycled Concrete Powder in Low-Carbon Ultra-High Performance Concrete (UHPC): Multi-Performance Evaluation. *Construction and Building Materials*, **441**, Article ID: 137520. https://doi.org/10.1016/j.conbuildmat.2024.137520

[9] Hou, S., Hu, R., Xu, L., Zhang, Y. and Ma, Z. (2024) Understanding the Chloride Migration in Recycled Powder Concrete: Effects of Recycled Powder Type, Replacement Rate and Substitution Pattern. *Construction and Building Materials*, **436**, Article ID: 136825. https://doi.org/10.1016/j.conbuildmat.2024.136825

[10] Liu, X., Liang, C., Zhang, Z., Zhang, Y., Xu, J. and Ma, Z. (2024) Mechanical Performance of Low-Carbon Ultra-High Performance Engineered Cementitious Composites (UHP-ECC) with High-Volume Recycled Concrete Powder. *Journal of Building Engineering*, **88**, Article ID: 109153. https://doi.org/10.1016/j.jobe.2024.109153

[11] Yu, P., Li, T. and Gao, S. (2024) Study on the Effect of Recycled Fine Powder on the Properties of Cement Mortar and Concrete. *Desalination and Water Treatment*, **319**, Article ID: 100481. https://doi.org/10.1016/j.dwt.2024.100481

[12] Singh, P. and Kapoor, K. (2024) Developing Geopolymer Concrete Using Fine Recycled Concrete Powder and Recycled Aggregates. *Magazine of Concrete Research*, **76**, 1091-1105. https://doi.org/10.1680/jmacr.23.00360

[13] Shen, Z., Zhu, H. and Meng, X. (2024) The Influence of Curing Methods on the Performance of Recycled Concrete Powder Artificial Aggregates and Concrete. *Construction and Building Materials*, **435**, Article ID: 136908. https://doi.org/10.1016/j.conbuildmat.2024.136908

[14] Kasulanati, M.L. and Pancharathi, R.K. (2021) Multi-Recycled Aggregate Concrete Towards a Sustainable Solution—A Review. *Cement Wapno Beton*, **26**, 35-45. https://doi.org/10.32047/cwb.2021.26.1.4

[15] FAO (2022) The State of World Fisheries and Aquaculture 2022.

[16] Ruslan, H.N., Muthusamy, K., Syed Mohsin, S.M., Jose, R. and Omar, R. (2022) Oyster Shell Waste as a Concrete Ingredient: A Review. *Materials Today: Proceedings*, **48**, 713-719. https://doi.org/10.1016/j.matpr.2021.02.208

[17] Song, Q., Wang, Q., Xu, S., Mao, J., Li, X. and Zhao, Y. (2022) Properties of Water-Repellent Concrete Mortar Containing Superhydrophobic Oyster Shell Powder. *Construction and Building Materials*, **337**, Article ID: 127423. https://doi.org/10.1016/j.conbuildmat.2022.127423

[18] Cha, I., Kim, J. and Lee, H. (2023) Enhancing Compressive Strength in Cementitious Composites through Effective Use of Wasted Oyster Shells and Admixtures. *Buildings*, **13**, Article 2787. https://doi.org/10.3390/buildings13112787

[19] Luo, K., Zhang, M., Jiang, Q., Wang, S. and Zhuo, X. (2024) Evaluation of Using Oyster Shell as a Complete Replacement for Aggregate to Make Eco-Friendly Concrete. *Journal of Building Engineering*, **84**, Article ID: 108587. https://doi.org/10.1016/j.jobe.2024.108587

[20] Jeon, J.H., Son, Y.H., Kim, T.J. and Jo, S.B. (2024) Engineering Performances of Permeable Concrete Blocks Using Oyster Shell, Bottom Ash, and Biochar. *Construction and Building Materials*, **440**, Article ID: 137374. https://doi.org/10.1016/j.conbuildmat.2024.137374

[21] Wan Mohammad, W.A.S.B., Othman, N.H., Wan Ibrahim, M.H., Rahim, M.A., Shahidan, S. and Rahman, R.A. (2017) A Review on Seashells Ash as Partial Cement Replacement. *IOP Conference Series*: *Materials Science and Engineering*, **271**, Article ID: 012059. https://doi.org/10.1088/1757-899x/271/1/012059

[22] Han, Y., Lin, R. and Wang, X. (2022) Performance of Sustainable Concrete Made from Waste Oyster Shell Powder and Blast Furnace Slag. *Journal of Building Engineering*, **47**, Article ID: 103918. https://doi.org/10.1016/j.jobe.2021.103918

[23] Miatto, A., Schandl, H., Fishman, T. and Tanikawa, H. (2016) Global Patterns and Trends for Non-Metallic Minerals Used for Construction. *Journal of Industrial Ecology*, **21**, 924-937. https://doi.org/10.1111/jiec.12471

[24] Liao, Y., Shi, H., Zhang, S., Da, B. and Chen, D. (2021) Particle Size Effect of Oyster Shell on Mortar: Experimental Investigation and Modeling. *Materials*, **14**, Article 6813. https://doi.org/10.3390/ma14226813

[25] Liao, Y., Wang, X., Kong, D., Da, B. and Chen, D. (2023) Experiment Research on Effect of Oyster Shell Particle Size on Mortar Transmission Properties. *Construction and Building Materials*, **375**, Article ID: 131012. https://doi.org/10.1016/j.conbuildmat.2023.131012

[26] Erdogdu, K., Tokyay, M. and Türker, P. (1999) Comparison of Intergrinding and Separate Grinding for the Production of Natural Pozzolan and GBFS-Incorporated Blended Cements. *Cement and Concrete Research*, **29**, 743-746. https://doi.org/10.1016/s0008-8846(99)00039-3

[27] Onaizi, A.M., Tang, W. and Liu, Y. (2024) Co-grinding Treatment for Developing Integrated-Properties SCMs from Basic Oxygen Furnace Slag and Furnace Bottom Ash: A Step toward Synthesis Advanced SCMs. *Case Studies in Construction Materials*, **20**, e03163. https://doi.org/10.1016/j.cscm.2024.e03163

[28] Dvořák, K., Dolák, D. and Dočkal, J. (2016) Comparison of Separate and Co-Grinding of the Blended Cements with the Pozzolanic Component. *Procedia Engineering*, **151**, 66-72. https://doi.org/10.1016/j.proeng.2016.07.376

[29] Maurya, S.K., Bhatrola, K. and Kothiyal, N.C. (2023) Sustainable Development of Mortar with Low Carbon Admixed High Volume Fly Ash. *Materials Today*: *Proceedings*, **93**, 428-435. https://doi.org/10.1016/j.matpr.2023.08.067

[30] Singh Kashyap, V., Agrawal, U., Arora, K. and Sancheti, G. (2021) FTIR Analysis of Nanomodified Cement Concrete Incorporating Nano Silica and Waste Marble Dust. *IOP Conference Series*: *Earth and Environmental Science*, **796**, Article ID: 012022. https://doi.org/10.1088/1755-1315/796/1/012022

[31] Ylmén, R., Jäglid, U., Steenari, B. and Panas, I. (2009) Early Hydration and Setting of Portland Cement Monitored by IR, SEM and Vicat Techniques. *Cement and Concrete Research*, **39**, 433-439. https://doi.org/10.1016/j.cemconres.2009.01.017

[32] Al Sekhaneh, W., Shiyyab, A., Arinat, M. and Gharaibeh, N. (2020) Use of Ftir and Thermogravimetric Analysis of Ancient Mortar from the Church of the Cross in Gerasa (Jordan) for Conservation Purposes. *Mediterranean Archaeology and Archaeometry*, **20**, 159-174.

[33] Santos, V.H.J.M.D., Pontin, D., Ponzi, G.G.D., Stepanha, A.S.D.G.E., Martel, R.B., Schütz, M.K., *et al.* (2021) Application of Fourier Transform Infrared Spectroscopy (FTIR) Coupled with Multivariate Regression for Calcium Carbonate ($CaCO_3$) Quantification in Cement. *Construction and Building Materials*, **313**, Article ID: 125413. https://doi.org/10.1016/j.conbuildmat.2021.125413

[34] Delgado, A.H., Paroli, R.M. and Beaudoin, J.J. (1996) Comparison of IR Techniques for the Characterization of Construction Cement Minerals and Hydrated Products. *Applied Spectroscopy*, **50**, 970-976. https://doi.org/10.1366/0003702963905312

[35] Bahari, A., Sadeghi-Nik, A., Roodbari, M., Sadeghi-Nik, A. and Mirshafiei, E. (2018) Experimental and Theoretical Studies of Ordinary Portland Cement Composites Contains Nano LSCO Perovskite with Fokker-Planck and Chemical Reaction Equations. *Construction and Building Materials*, **163**, 247-255. https://doi.org/10.1016/j.conbuildmat.2017.12.073

[36] Nukah, P.D., Abbey, S.J., Booth, C.A. and Oti, J. (2024) Development of Low Carbon Concrete and Prospective of Geopolymer Concrete Using Lightweight Coarse Aggregate and Cement Replacement Materials. *Construction and Building Materials*, **428**, Article ID: 136295. https://doi.org/10.1016/j.conbuildmat.2024.136295

[37] Kunther, W., Ferreiro, S. and Skibsted, J. (2017) Influence of the Ca/Si Ratio on the Compressive Strength of Cementitious Calcium-Silicate-Hydrate Binders. *Journal of Materials Chemistry A*, **5**, 17401-17412. https://doi.org/10.1039/c7ta06104h

[38] Dinh, H.L., Liu, J., Doh, J. and Ong, D.E.L. (2024) Influence of Si/Al Molar Ratio and Ca Content on the Performance of Fly Ash-Based Geopolymer Incorporating Waste Glass and GGBFs. *Construction and Building Materials*, **411**, Article ID: 134741. https://doi.org/10.1016/j.conbuildmat.2023.134741